Supplementary Material

Structural Effects of Composition Tuning in A-Site Disordered Perovskite $La_{0.5}M_{0.5}TiO_3$ (M = Li, Na, K) Nanorods for Fast Interfacial Transport for Solid Composite Electrolyte Design

*Lauren B. Shepard[1], Albina Borisevich[2], Tao Wang[3,4], Jiyoung Ock[3], Alexei P. Sokolov[3,4], X. Chelsea Chen[3], Sheng Dai[3,4], *Susan B. Sinnott[1,5,6,7]

[1]*Department of Materials Science and Engineering, The Pennsylvania State University, University Park, PA, 16802 USA*
[2]*Center for Nanophase Materials Sciences, Oak Ridge National Laboratory, Oak Ridge, TN, 37831 USA*
[3]*Chemical Sciences Division, Oak Ridge National Laboratory, Oak Ridge, TN, 37830 USA*
[4]*Department of Chemistry, Institute for Advanced Materials and Manufacturing, University of Tennessee, Knoxville, TN, 37996 USA*
[5]*Department of Chemistry, The Pennsylvania State University, University Park, PA, 16802 USA*
[6]*Institute for Computational and Data Sciences, The Pennsylvania State University, University Park, PA, 16802 USA*
[7]*Materials Research Institute, The Pennsylvania State University, University Park, PA, 16802 USA*

***Corresponding Authors:** Lauren B. Shepard (lzs5735@psu.edu) and Susan B. Sinnott (sbs5563@psu.edu)

Table of Contents

Orthorhombic and Cubic Perovskite Crystal Structure

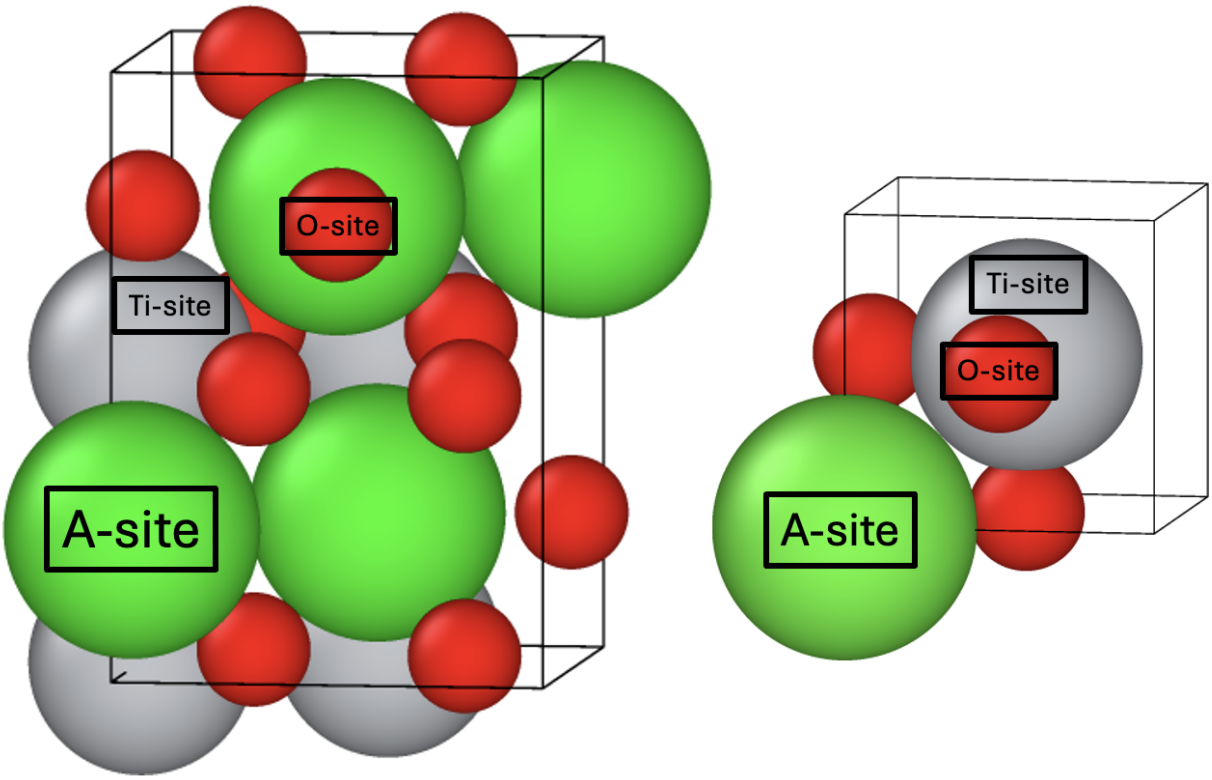

Figure S1. (Left) Orthorhombic (Pnma) and (right) pseudocubic (P4/mmm) perovskite $ATiO_3$ unit cell with atom positions labeled; crystal structure obtained from Materials Project and ICSD and Ovito used for visualization.[30–46]

PAW Pseudopotentials Used in DFT Calculations

Table S1. List of PAW Pseudopotentials (POTCAR) Used in DFT Calculations for Each Atom Species in the Input Structures

Element	POTCAR Symbol
Li	Li_sv
La	La
Ti	Ti_pv
O	O
C	C
N	N
F	F
H	H
S	S
Na	Na_pv
K	K_sv

Bond length Distributions from Bulk Pseudocubic Calculations

x = 0

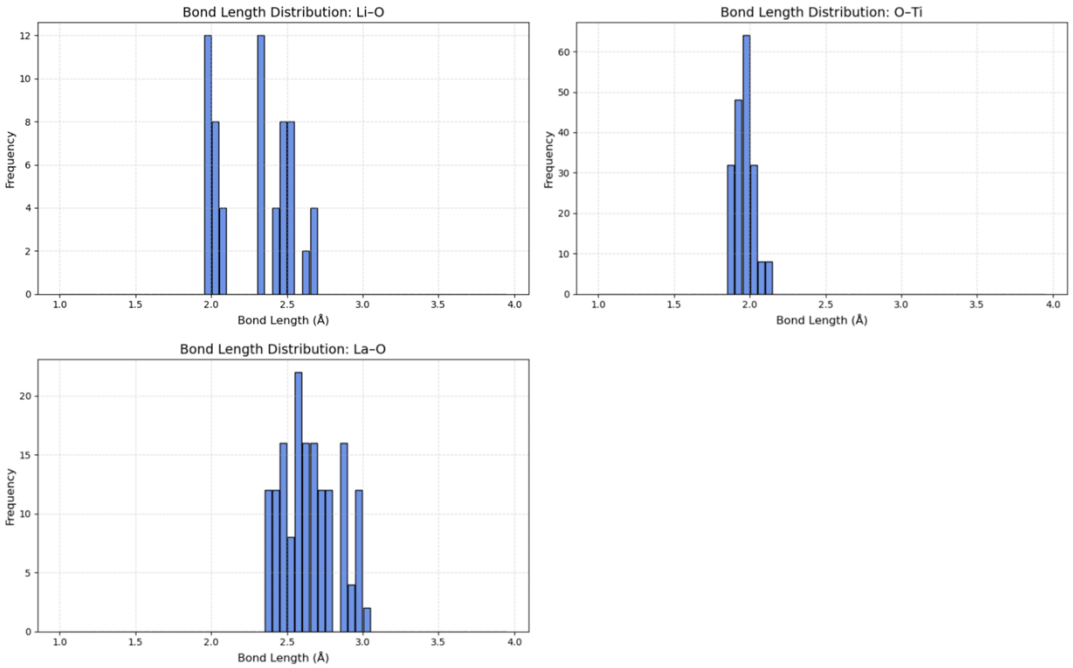

Figure S2. Bond length distributions for Li-O, La-O, and Ti-O for bulk pseudocubic $Li_{0.5}La_{0.5}TiO_3$.

x = 0.0625 (K)

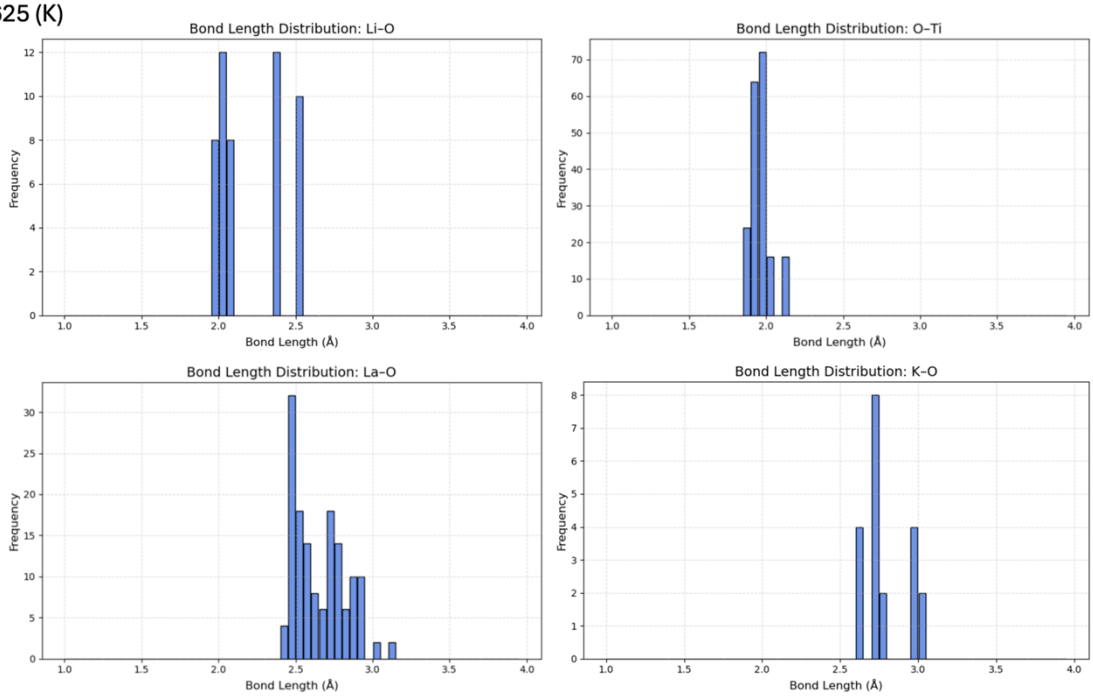

Figure S3. Bond length distributions for Li-O, K-O, La-O, and Ti-O for bulk pseudocubic $Li_{0.4375}K_{0.0625}La_{0.5}TiO_3$.

x = 0.125 (K)

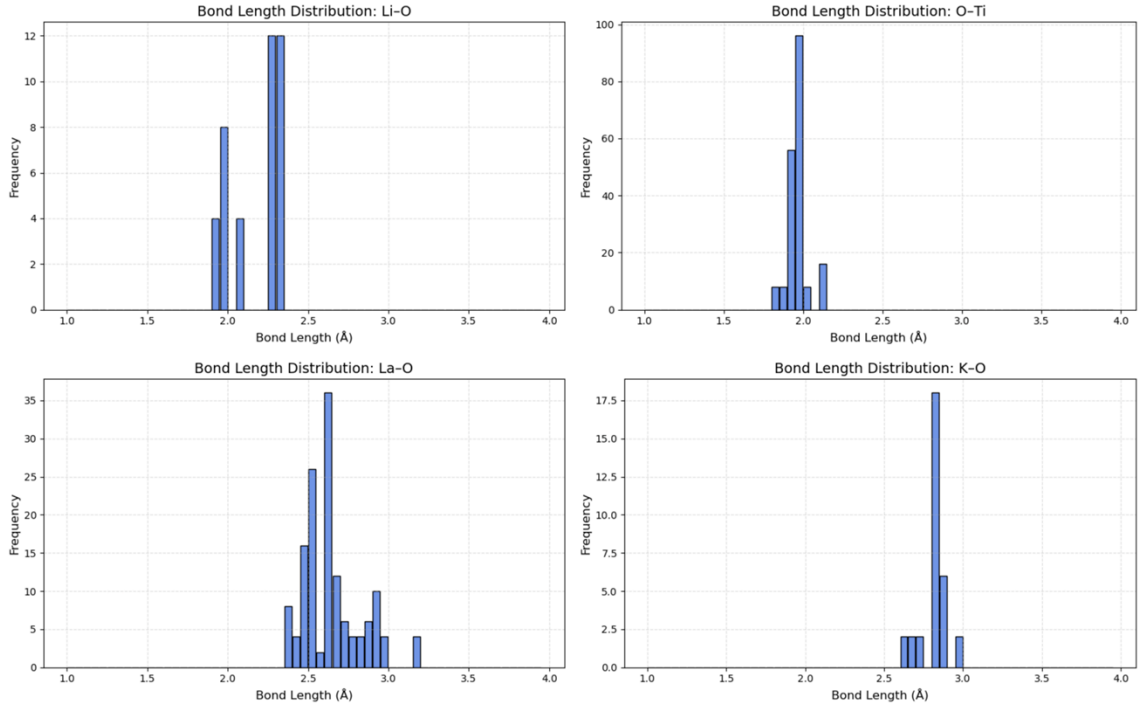

Figure S4. Bond length distributions for Li-O, K-O, La-O, and Ti-O for bulk pseudocubic $Li_{0.375}K_{0.125}La_{0.5}TiO_3$.

x = 0.1875 (K)

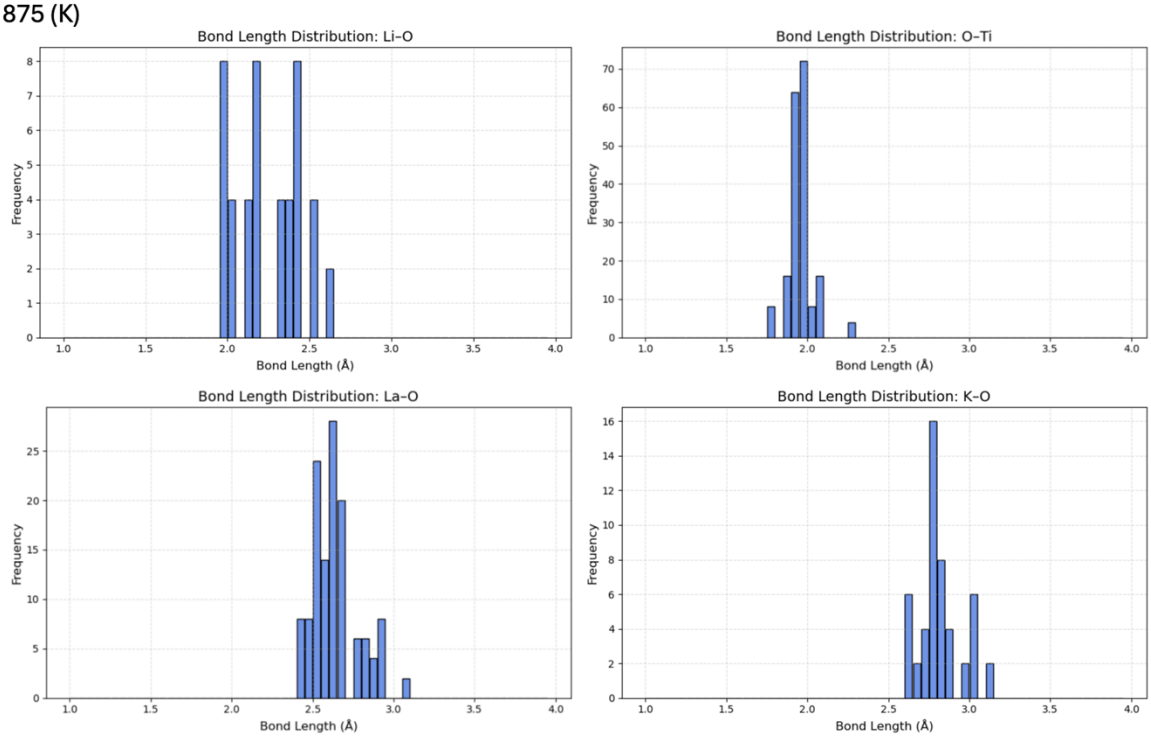

Figure S5. Bond length distributions for Li-O, K-O, La-O, and Ti-O for bulk pseudocubic $Li_{0.3125}K_{0.1875}La_{0.5}TiO_3$.

x = 0.25 (K)

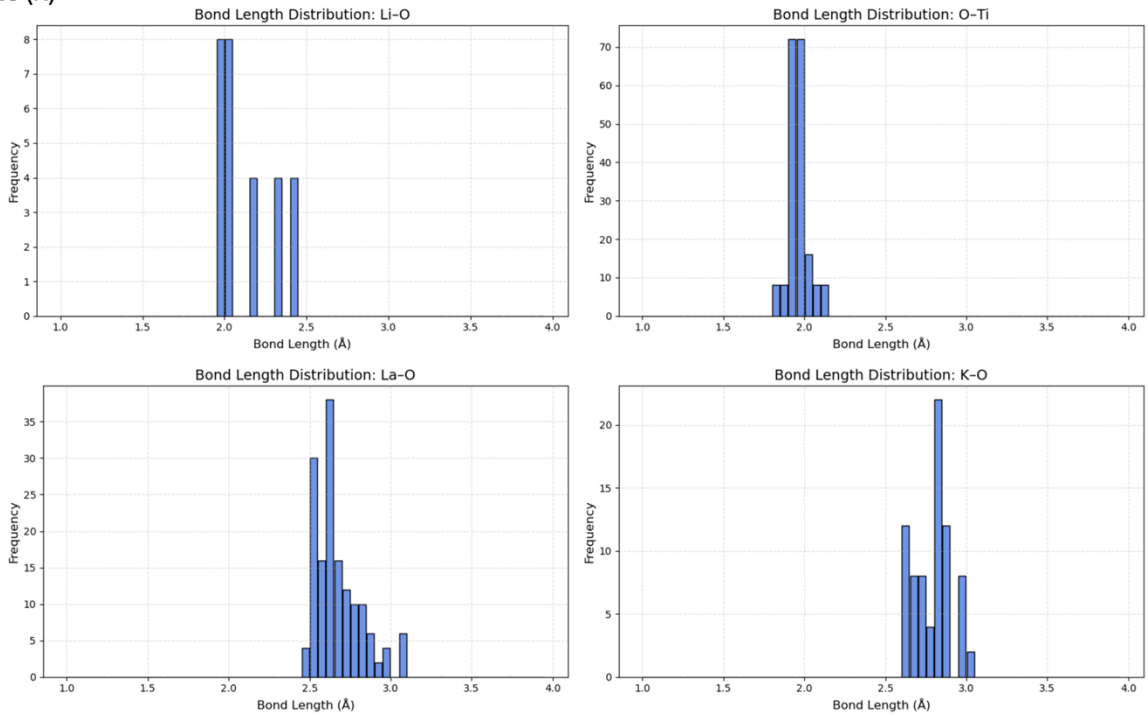

Figure S6. Bond length distributions for Li-O, K-O, La-O, and Ti-O for bulk pseudocubic $Li_{0.25}K_{0.25}La_{0.5}TiO_3$.

x = 0.3125 (K)

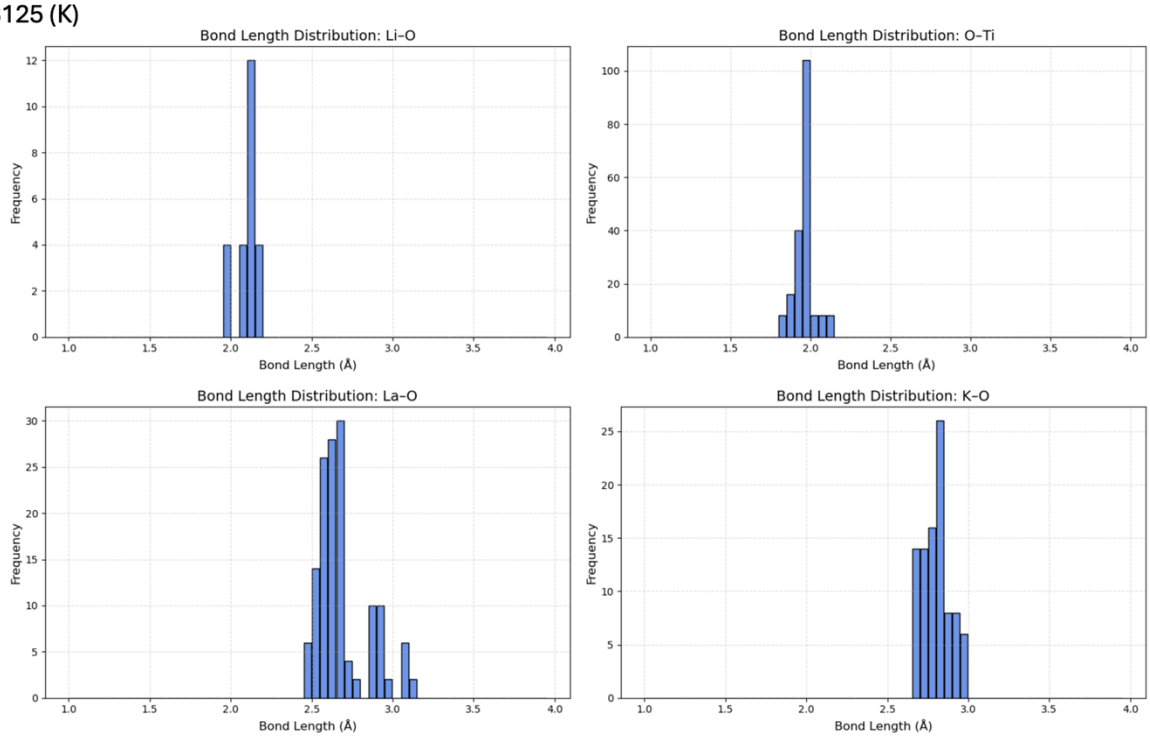

Figure S7. Bond length distributions for Li-O, K-O, La-O, and Ti-O for bulk pseudocubic $Li_{0.1875}K_{0.3125}La_{0.5}TiO_3$.

x = 0.50 (K)

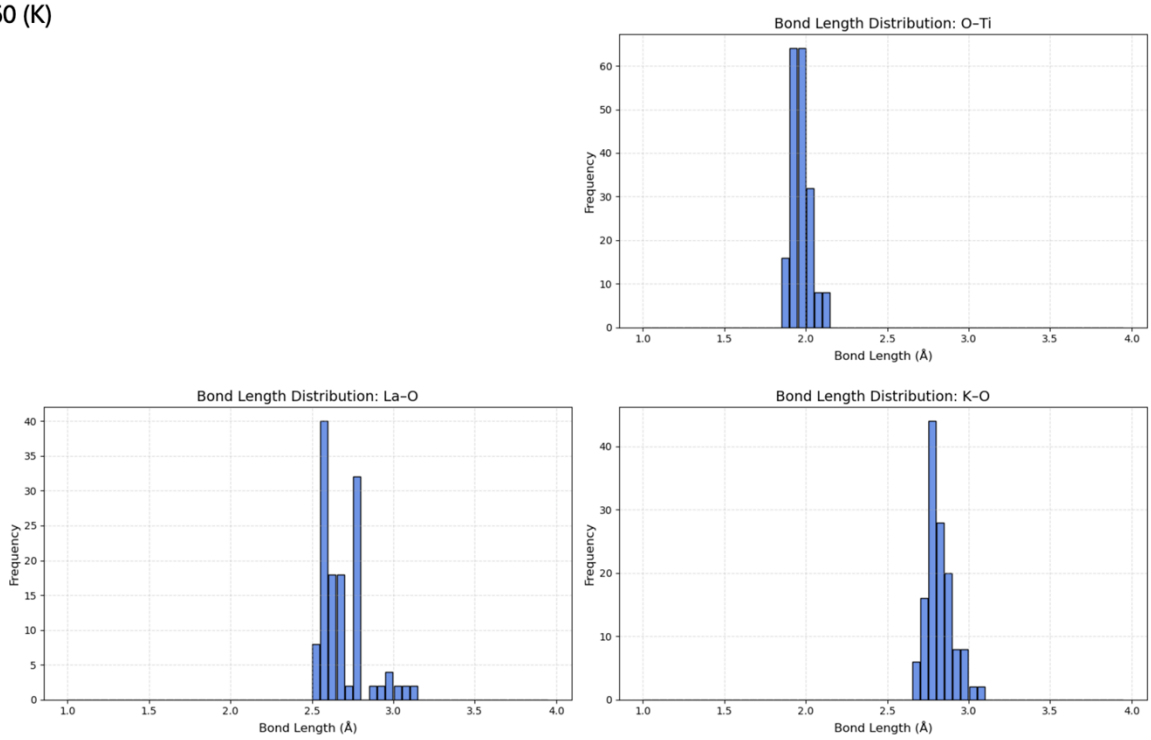

Figure S8. Bond length distributions for K-O, La-O, and Ti-O for bulk pseudocubic $K_{0.5}La_{0.5}TiO_3$.

x = 0.0625 (Na)

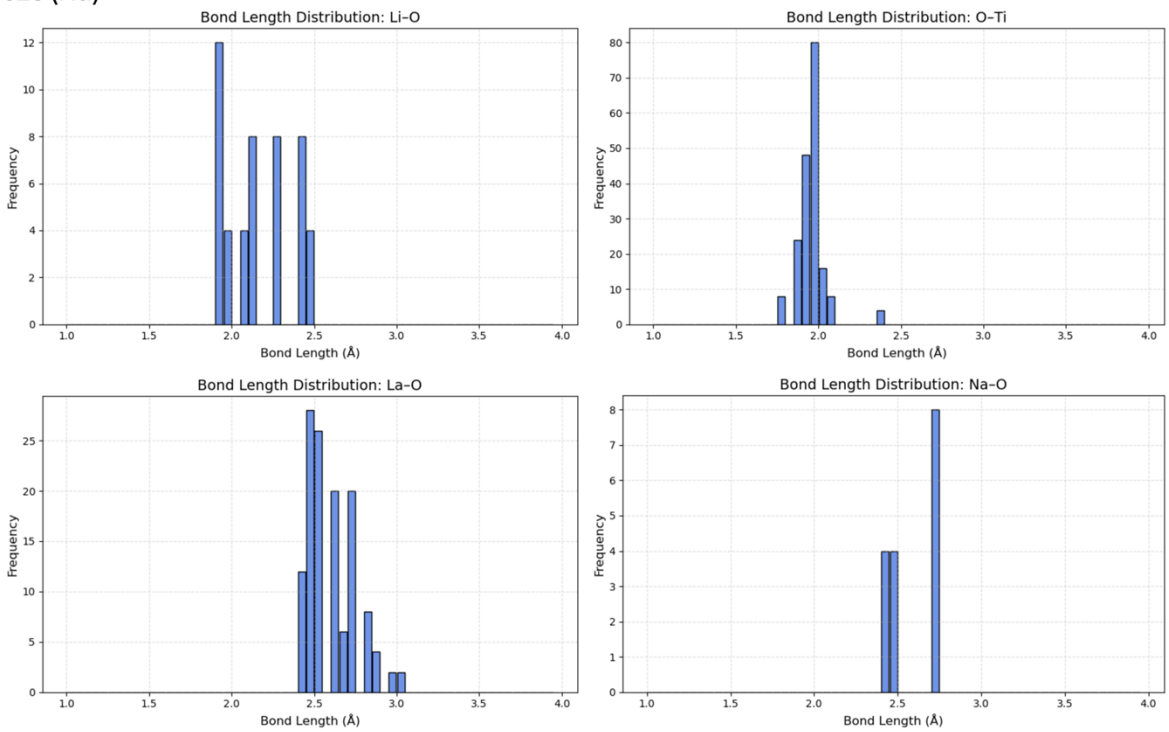

Figure S9. Bond length distributions for Li-O, Na-O, La-O, and Ti-O for bulk pseudocubic $Li_{0.4375}Na_{0.0625}La_{0.5}TiO_3$.

x = 0.125 (Na)

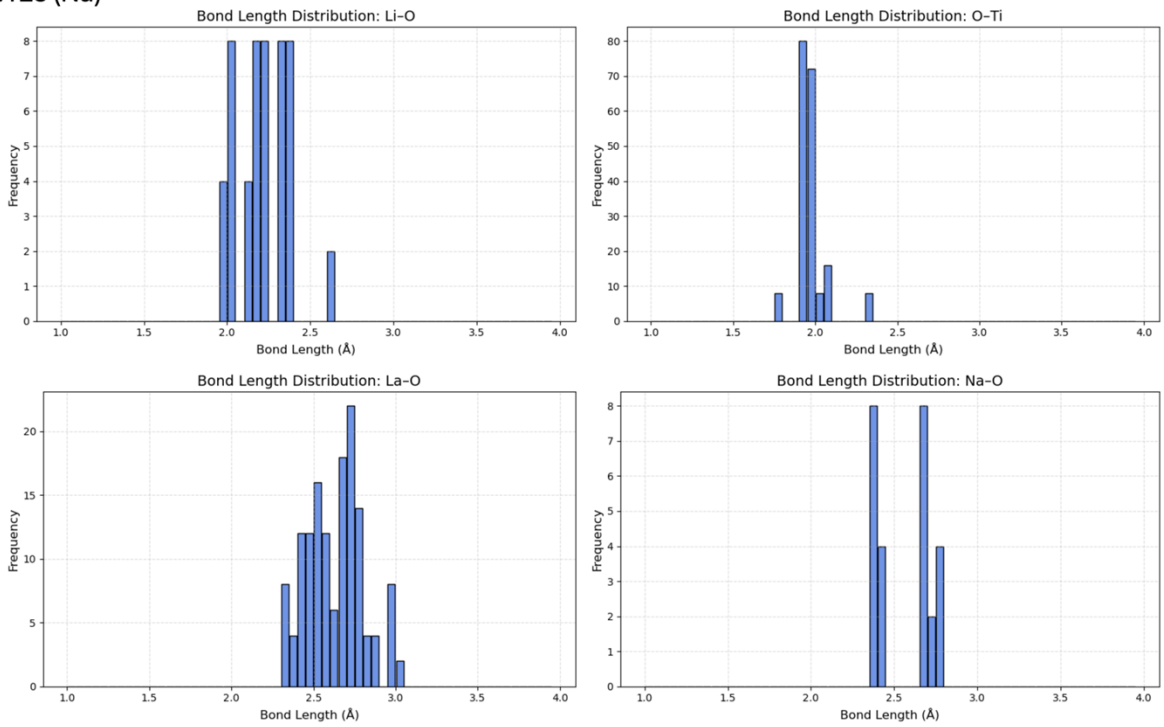

Figure S10. Bond length distributions for Li-O, Na-O, La-O, and Ti-O for bulk pseudocubic $Li_{0.375}Na_{0.125}La_{0.5}TiO_3$.

x = 0.1875 (Na)

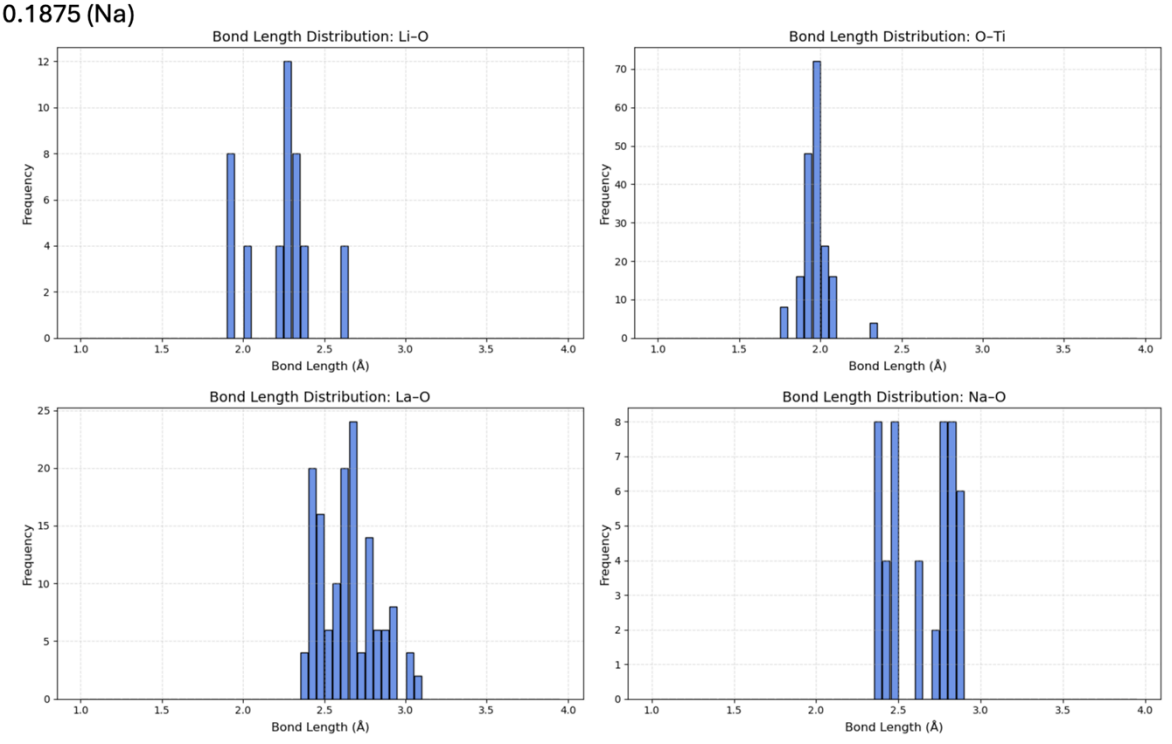

Figure S11. Bond length distributions for Li-O, Na-O, La-O, and Ti-O for bulk pseudocubic $Li_{0.3125}Na_{0.1875}La_{0.5}TiO_3$.

x = 0.25 (Na)

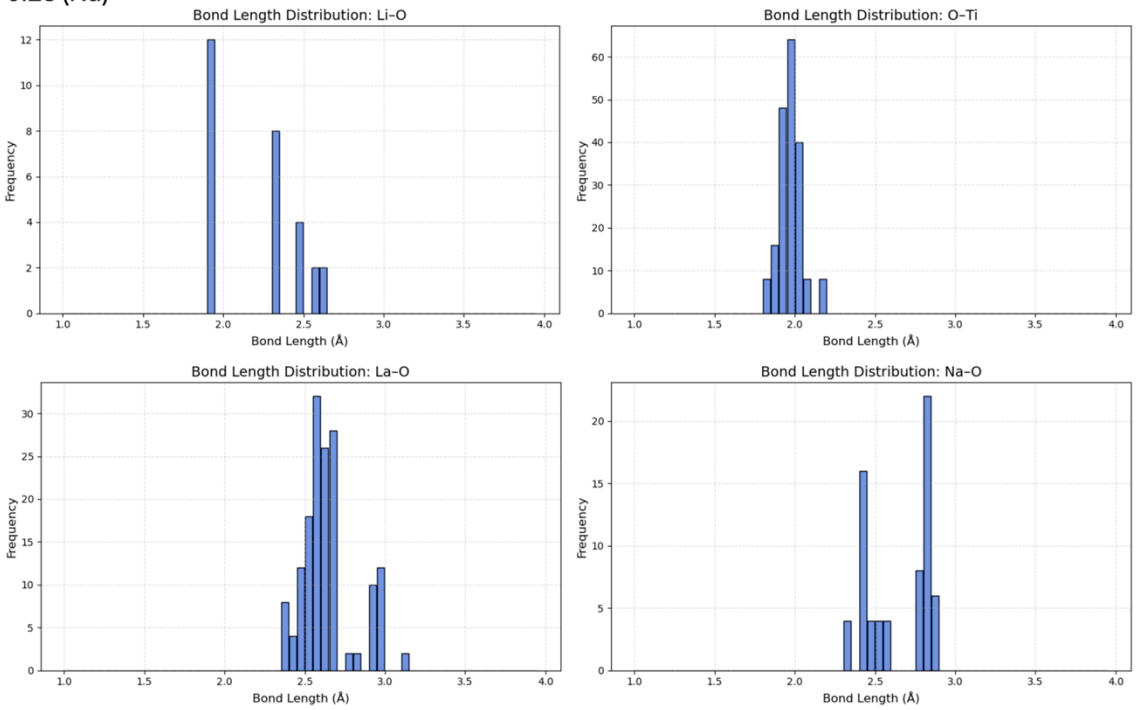

Figure S12. Bond length distributions for Li-O, Na-O, La-O, and Ti-O for bulk pseudocubic $Li_{0.25}Na_{0.25}La_{0.5}TiO_3$.

x = 0.3125 (Na)

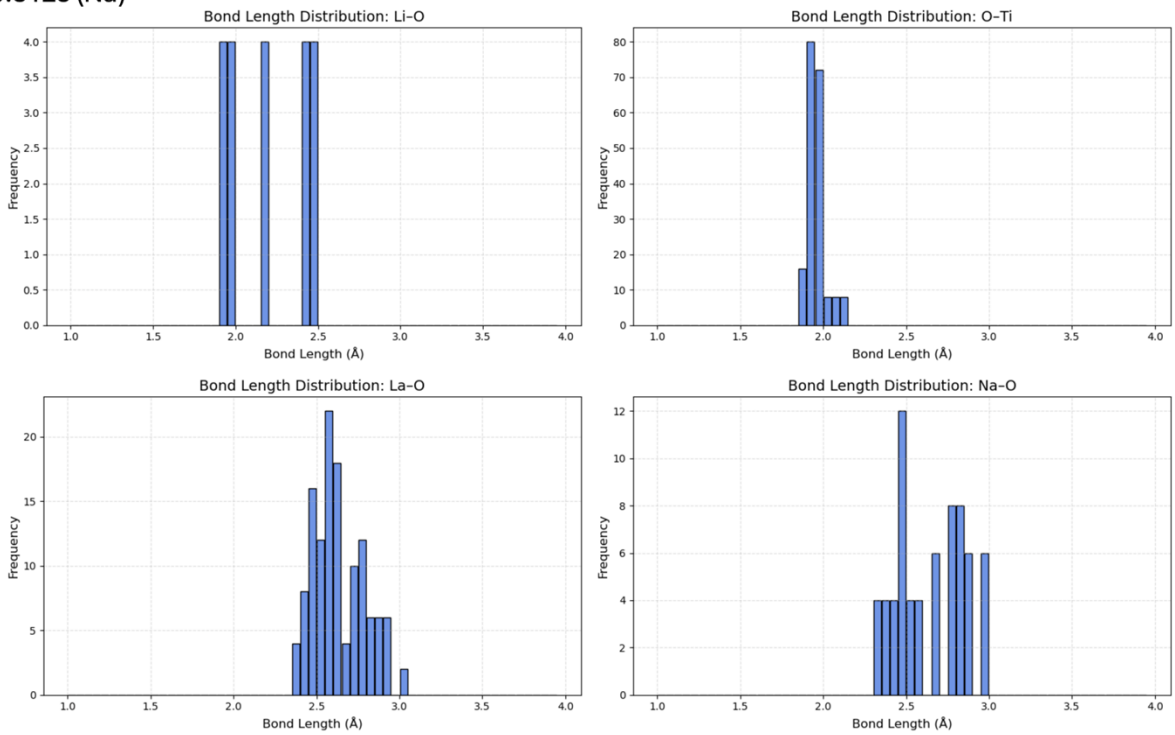

Figure S13. Bond length distributions for Li-O, Na-O, La-O, and Ti-O for bulk pseudocubic $Li_{0.1875}Na_{0.3125}La_{0.5}TiO_3$.

x = 0.50 (Na)

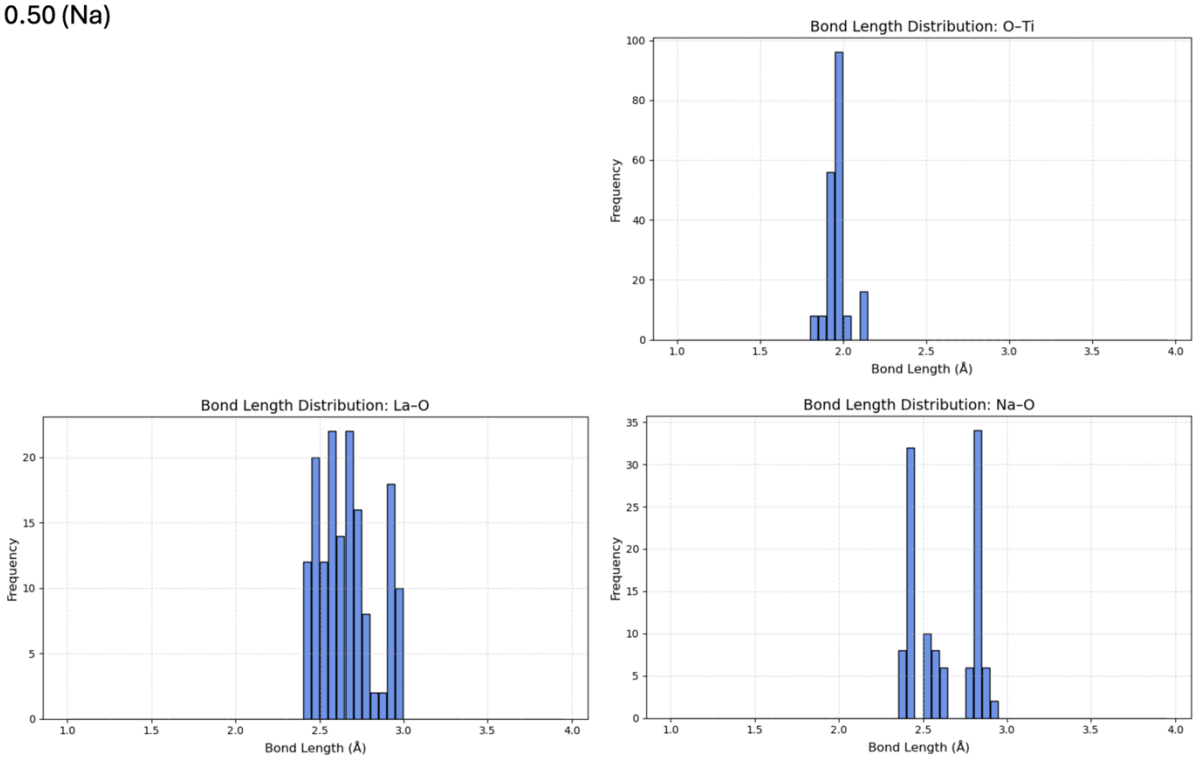

Figure S14. Bond length distributions for Na-O, La-O, and Ti-O for bulk pseudocubic $Na_{0.5}La_{0.5}TiO_3$.

Average Bond Lengths from Bulk Pseudocubic Calculations

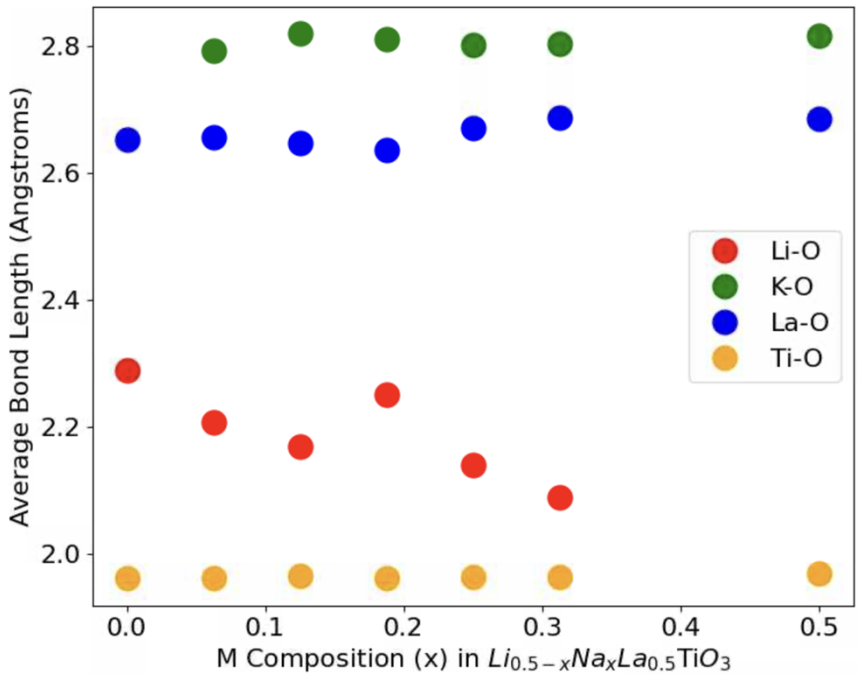

Figure S15. Average bond lengths for Li-O, K-O, La-O, and Ti-O from bulk pseudocubic calculations for $Li_{0.5-x}K_xLa_{0.5}TiO_3$, with x varying from 0 to 0.3125.

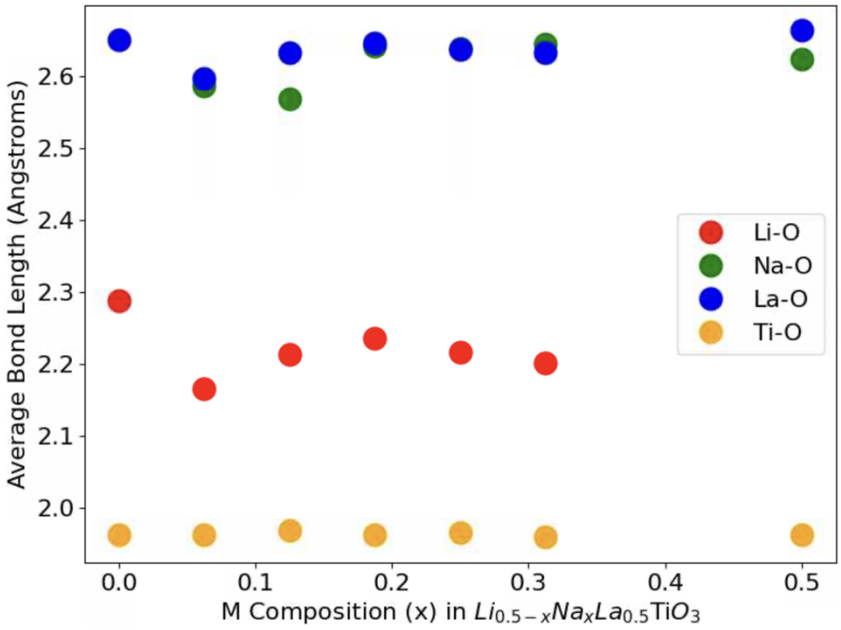

Figure S16. Average bond lengths for Li-O, Na-O, La-O, and Ti-O from bulk pseudocubic calculations for $Li_{0.5-x}Na_xLa_{0.5}TiO_3$, with x varying from 0 to 0.3125.

Bond Length Distributions from Surface Calculations

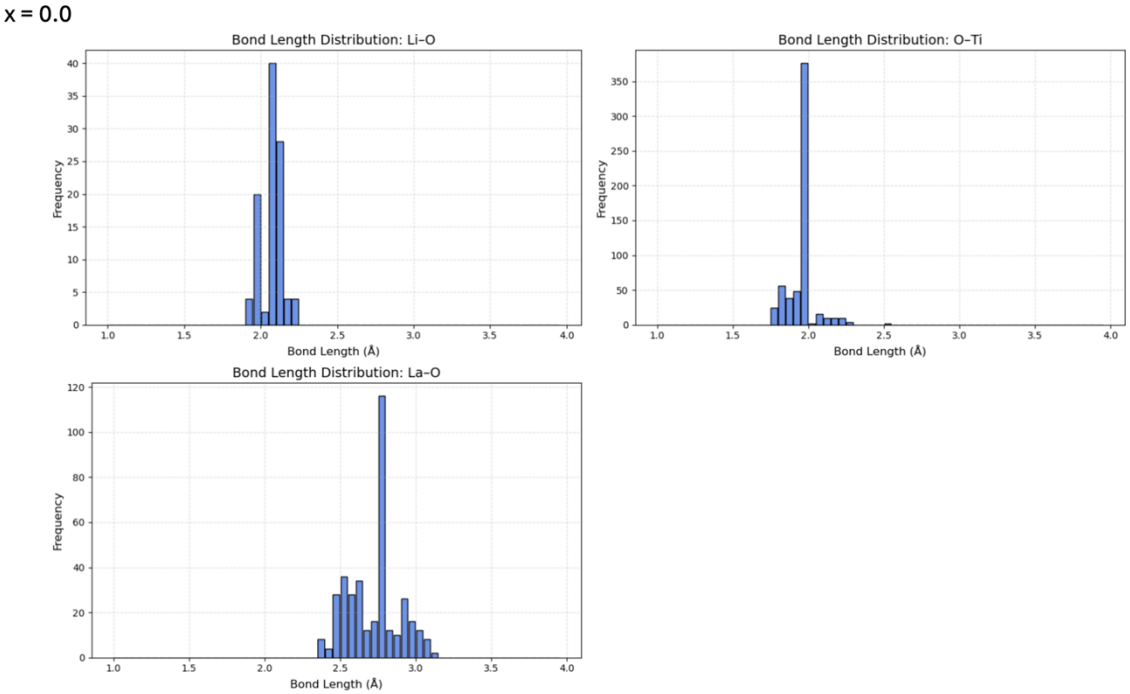

Figure S17. Bond length distributions for Li-O, La-O, and Ti-O for surface pseudocubic $Li_{0.5}La_{0.5}TiO_3$.

x = 0.0625 (K)

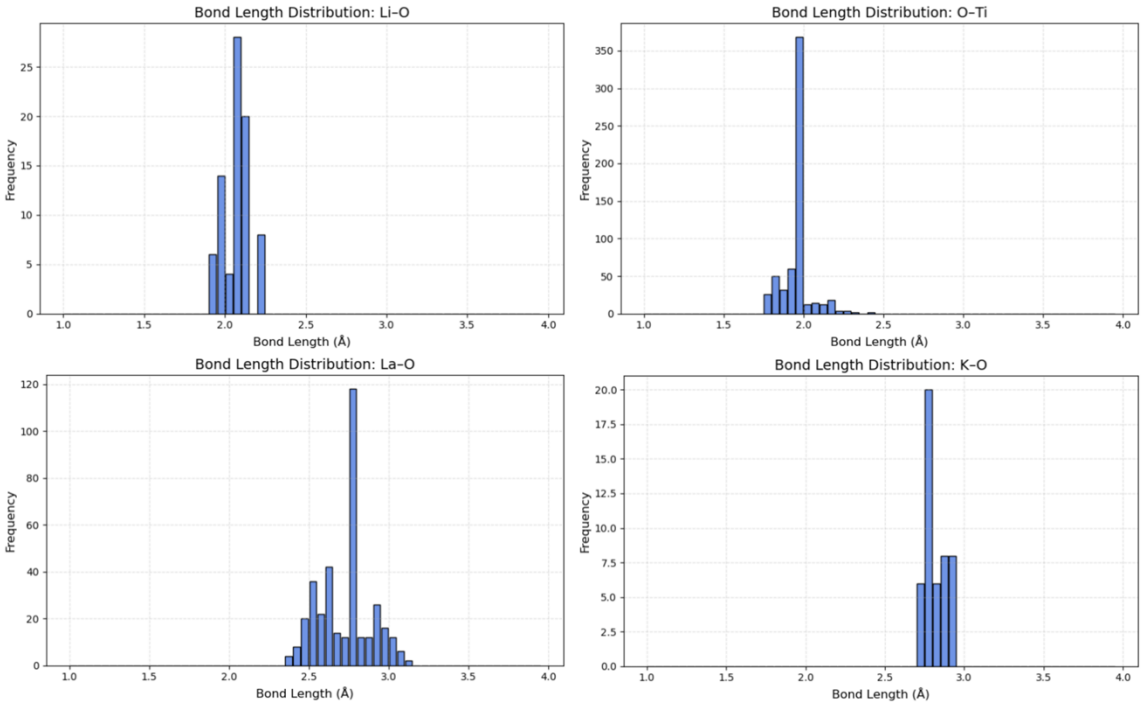

Figure S18. Bond length distributions for Li-O, K-O, La-O, and Ti-O for surface pseudocubic $Li_{0.4375}K_{0.0625}La_{0.5}TiO_3$.

x = 0.125 (K)

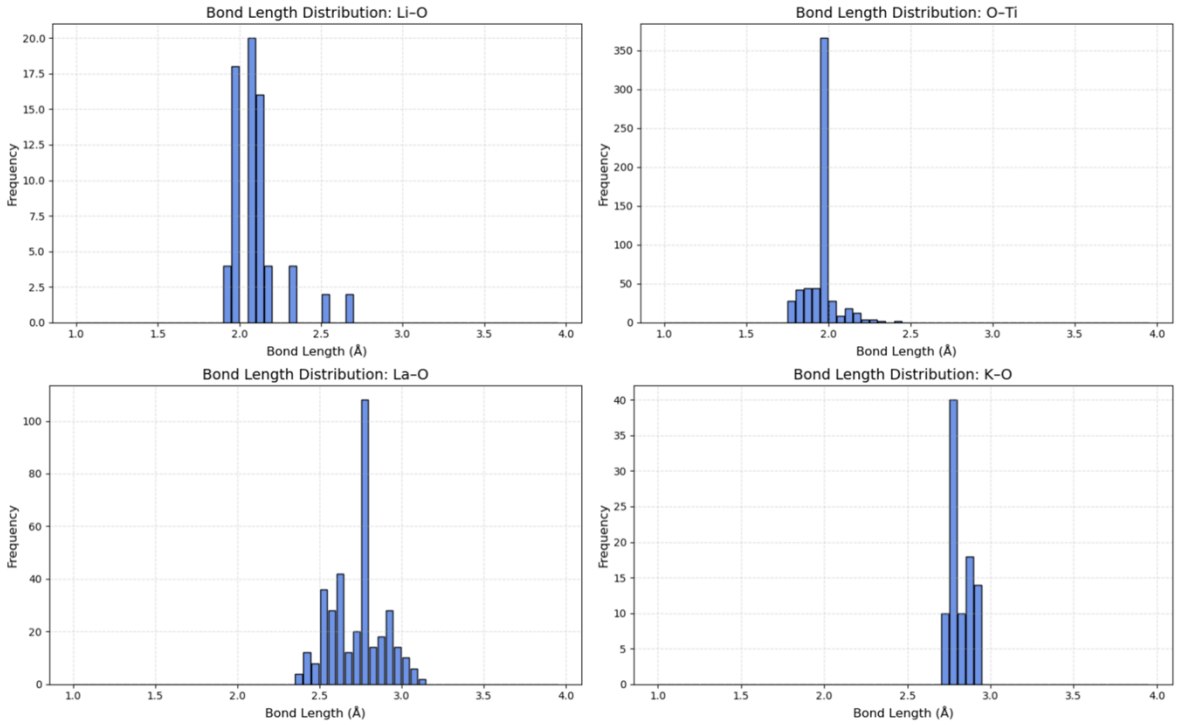

Figure S19. Bond length distributions for Li-O, K-O, La-O, and Ti-O for surface pseudocubic $Li_{0.375}K_{0.125}La_{0.5}TiO_3$.

x = 0.1875 (K)

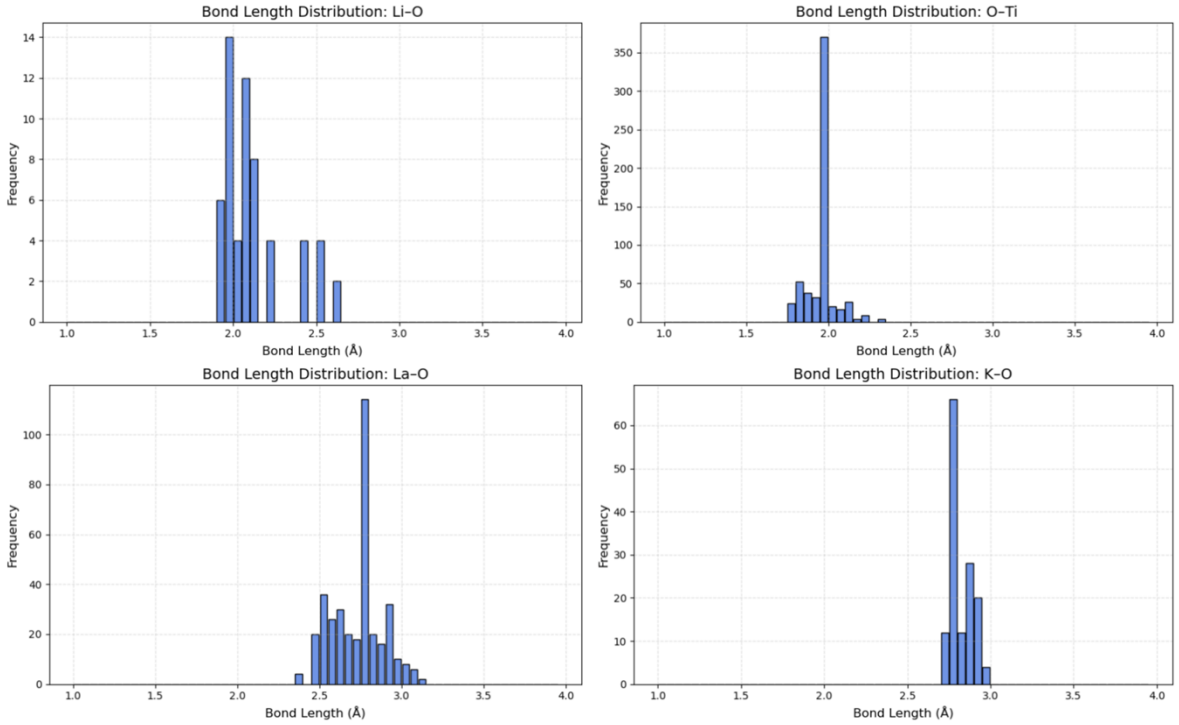

Figure S20. Bond length distributions for Li-O, K-O, La-O, and Ti-O for surface pseudocubic $Li_{0.3125}K_{0.1875}La_{0.5}TiO_3$.

x = 0.25 (K)

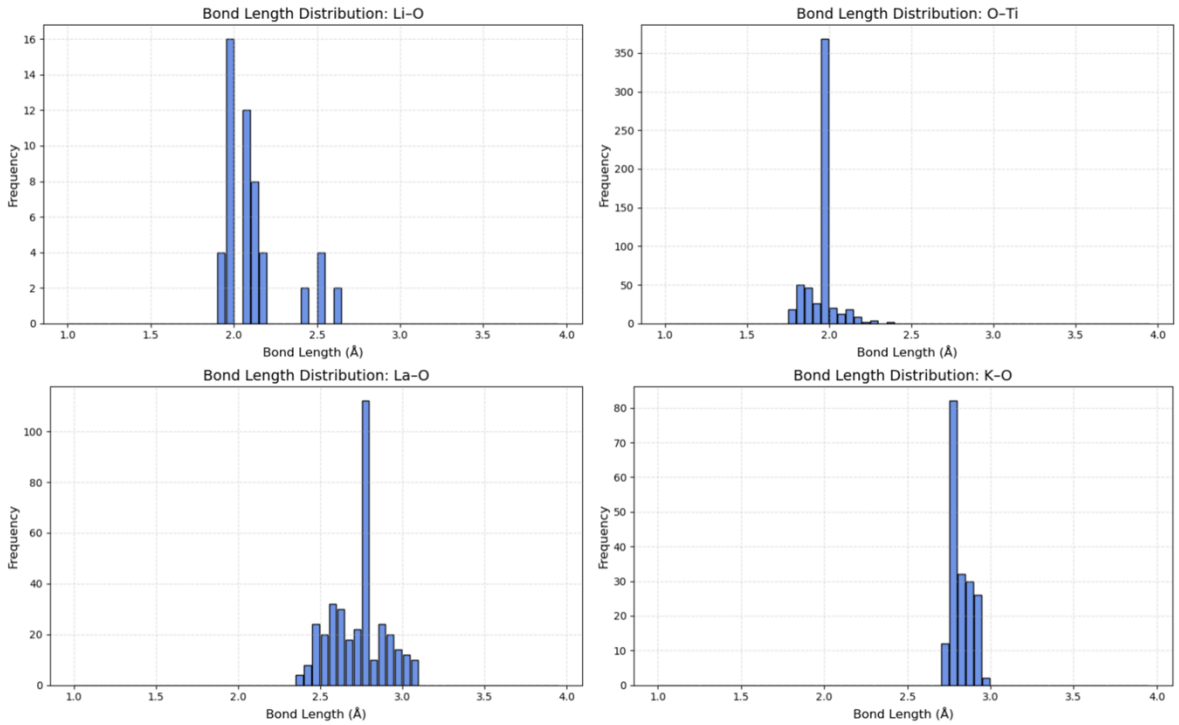

Figure S21. Bond length distributions for Li-O, K-O, La-O, and Ti-O for surface pseudocubic $Li_{0.25}K_{0.25}La_{0.5}TiO_3$.

x = 0.3125 (K)

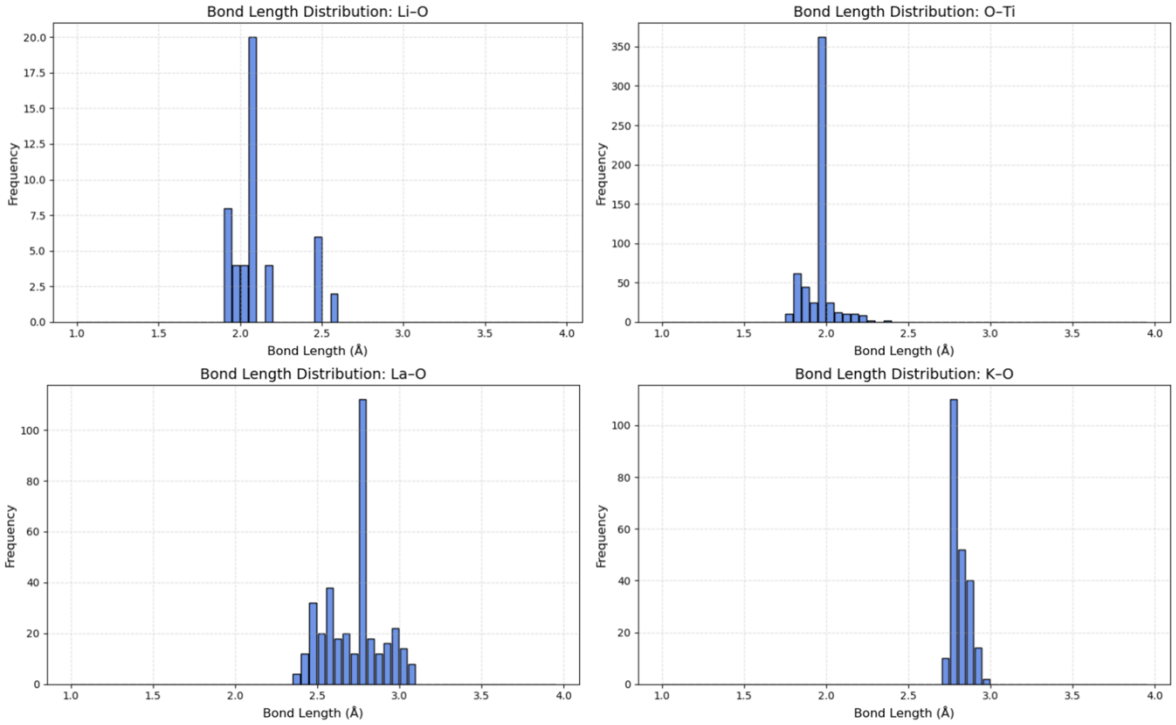

Figure S22. Bond length distributions for Li-O, K-O, La-O, and Ti-O for surface pseudocubic $Li_{0.1875}K_{0.3125}La_{0.5}TiO_3$.

x = 0.375 (K)

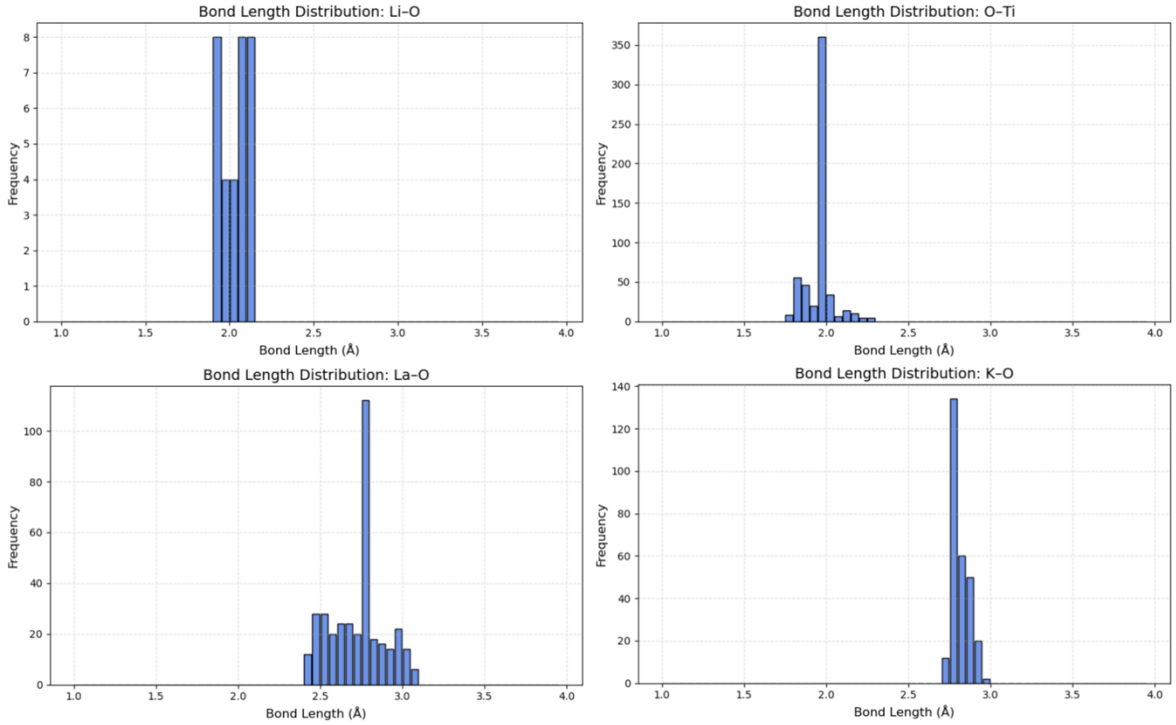

Figure S23. Bond length distributions for Li-O, K-O, La-O, and Ti-O for surface pseudocubic $Li_{0.125}K_{0.375}La_{0.5}TiO_3$.

x = 0.50 (K)

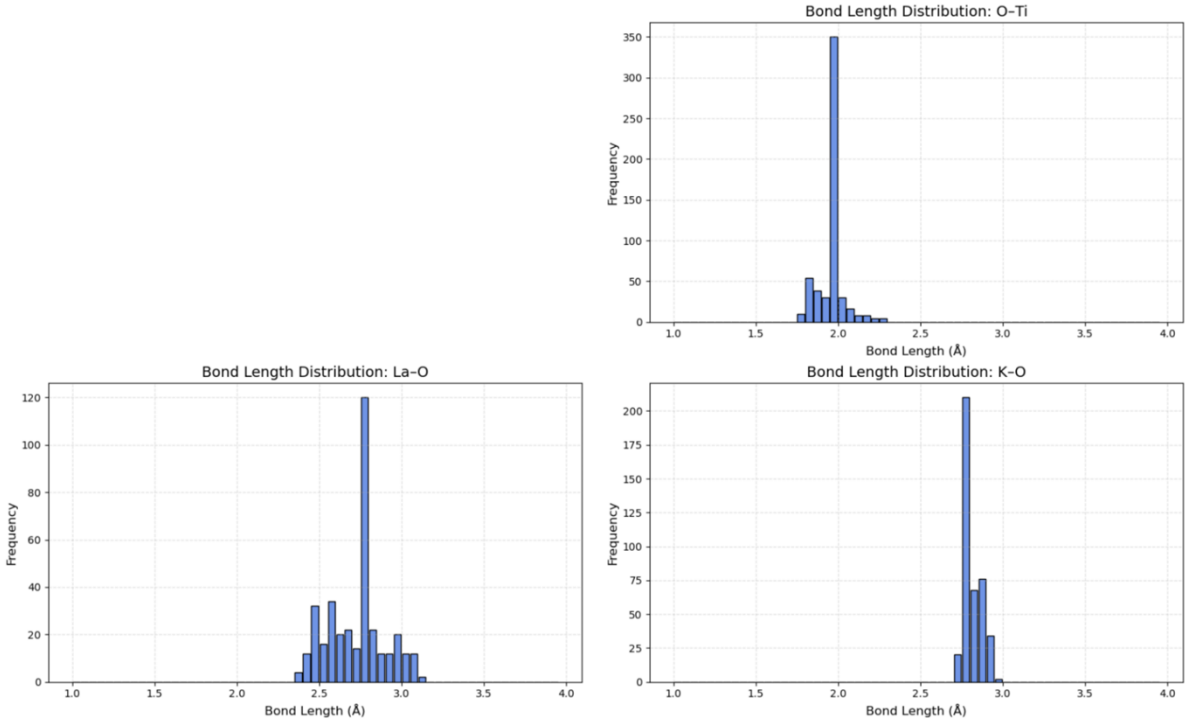

Figure 24. Bond length distributions for K-O, La-O, and Ti-O for surface pseudocubic $K_{0.5}La_{0.5}TiO_3$.

x = 0.0625 (Na)

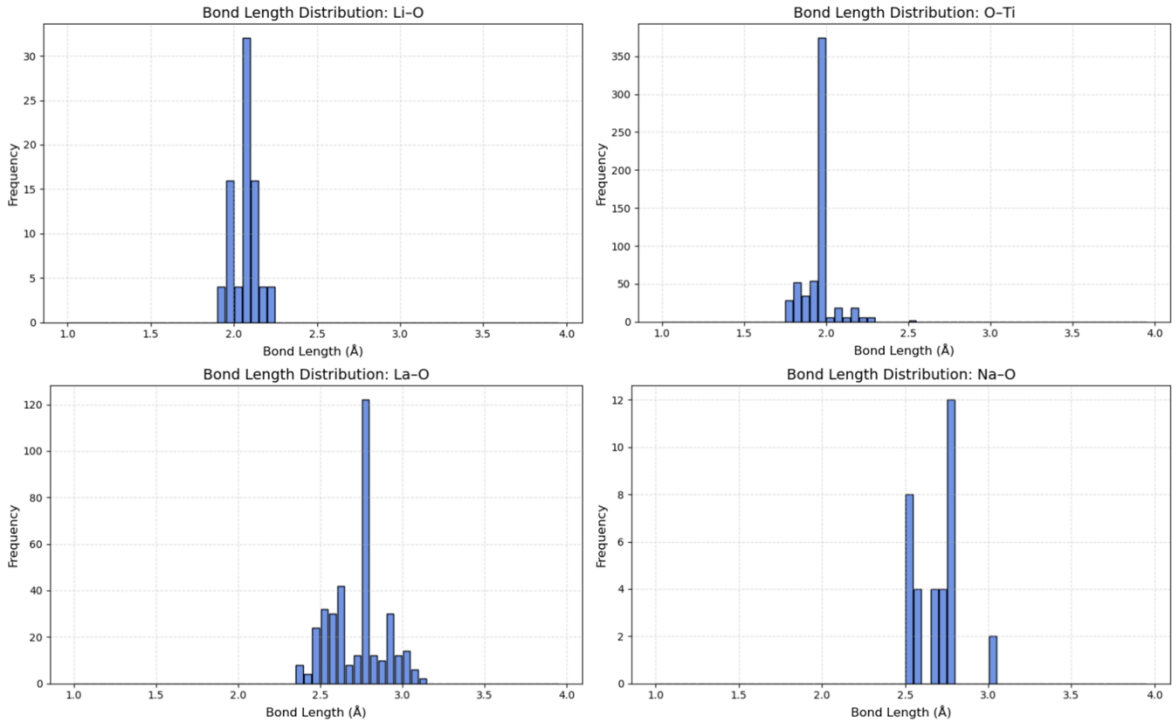

Figure S25. Bond length distributions for Li-O, Na-O, La-O, and Ti-O for surface pseudocubic $Li_{0.3175}Na_{0.0625}La_{0.5}TiO_3$.

x = 0.125 (Na)

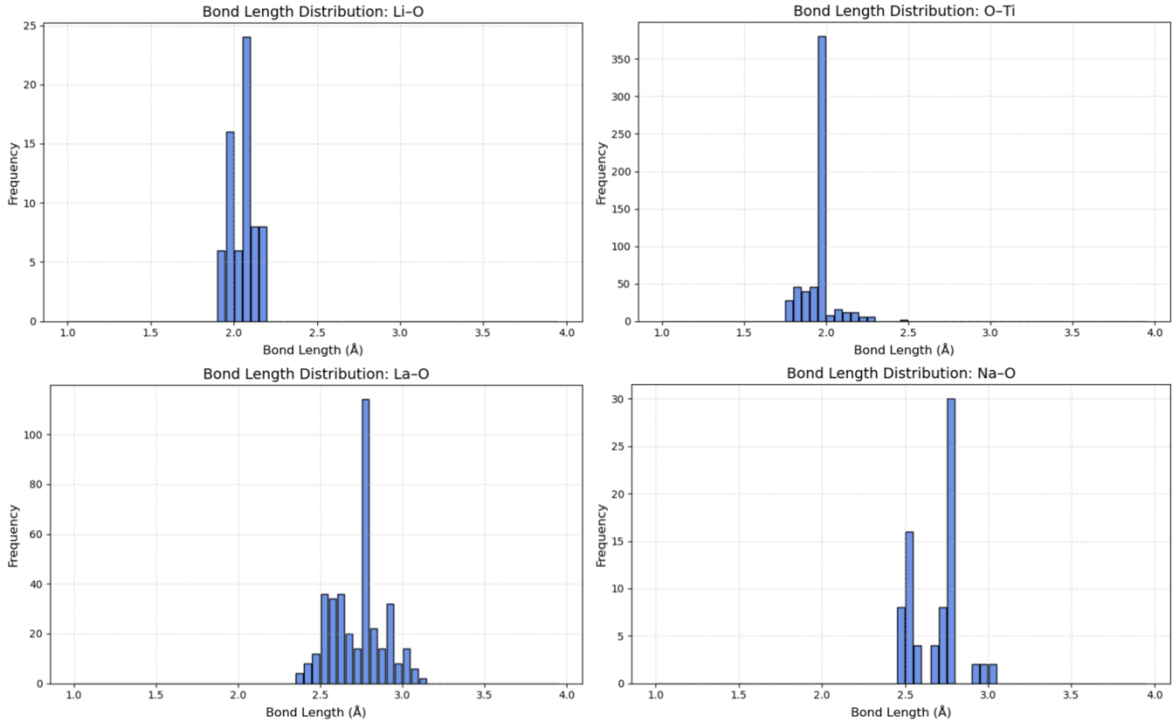

Figure S26. Bond length distributions for Li-O, Na-O, La-O, and Ti-O for surface pseudocubic $Li_{0.375}Na_{0.125}La_{0.5}TiO_3$.

x = 0.1875 (Na)

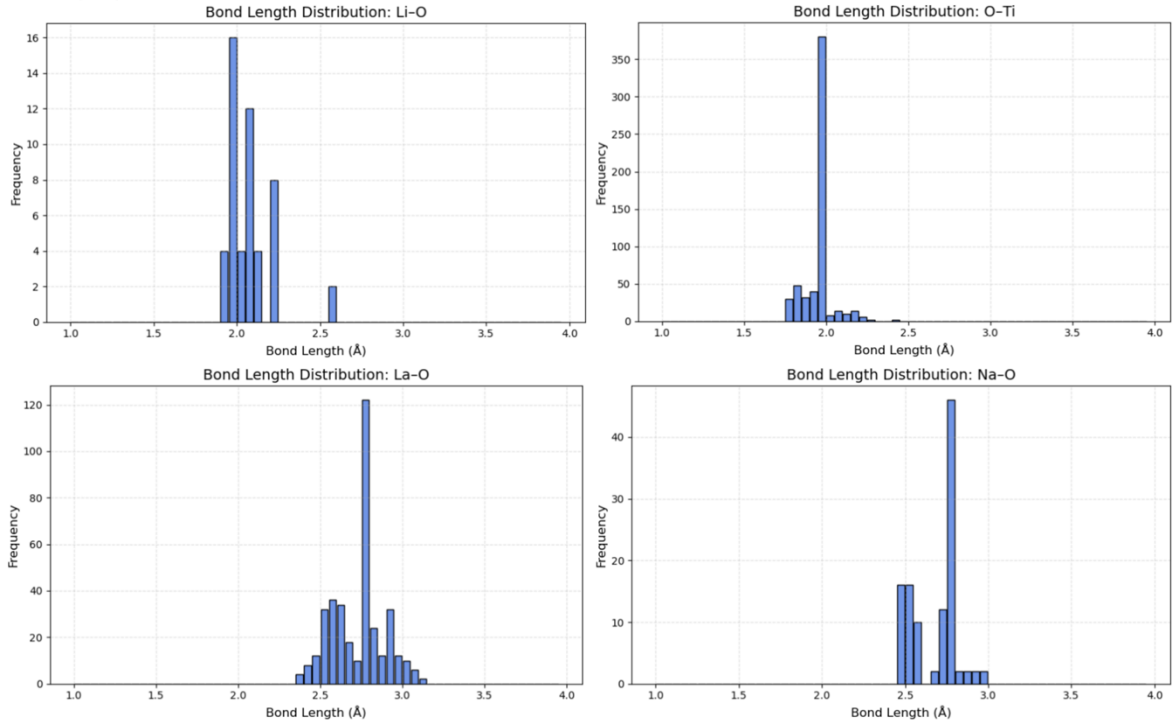

Figure S27. Bond length distributions for Li-O, Na-O, La-O, and Ti-O for surface pseudocubic $Li_{0.3125}Na_{0.1875}La_{0.5}TiO_3$.

x = 0.25 (Na)

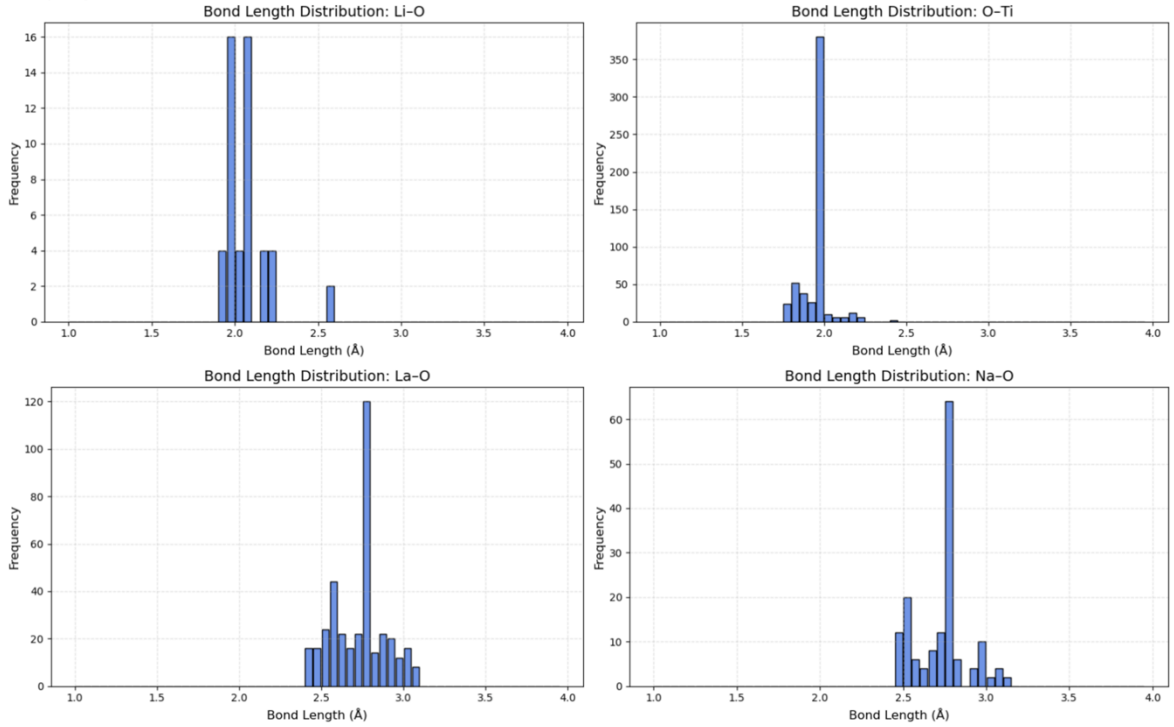

Figure S28. Bond length distributions for Li-O, Na-O, La-O, and Ti-O for surface pseudocubic $Li_{0.25}Na_{0.25}La_{0.5}TiO_3$.

x = 0.3125 (Na)

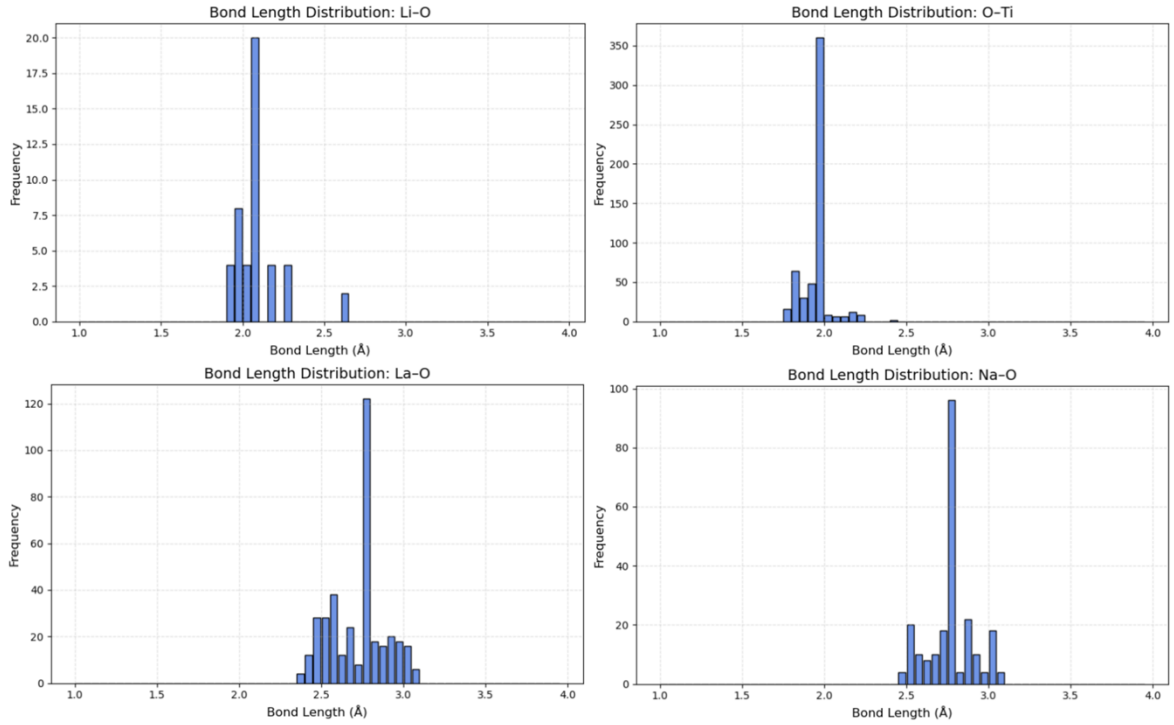

Figure S29. Bond length distributions for Li-O, Na-O, La-O, and Ti-O for surface pseudocubic $Li_{0.1875}Na_{0.3125}La_{0.5}TiO_3$.

x = 0.375 (Na)

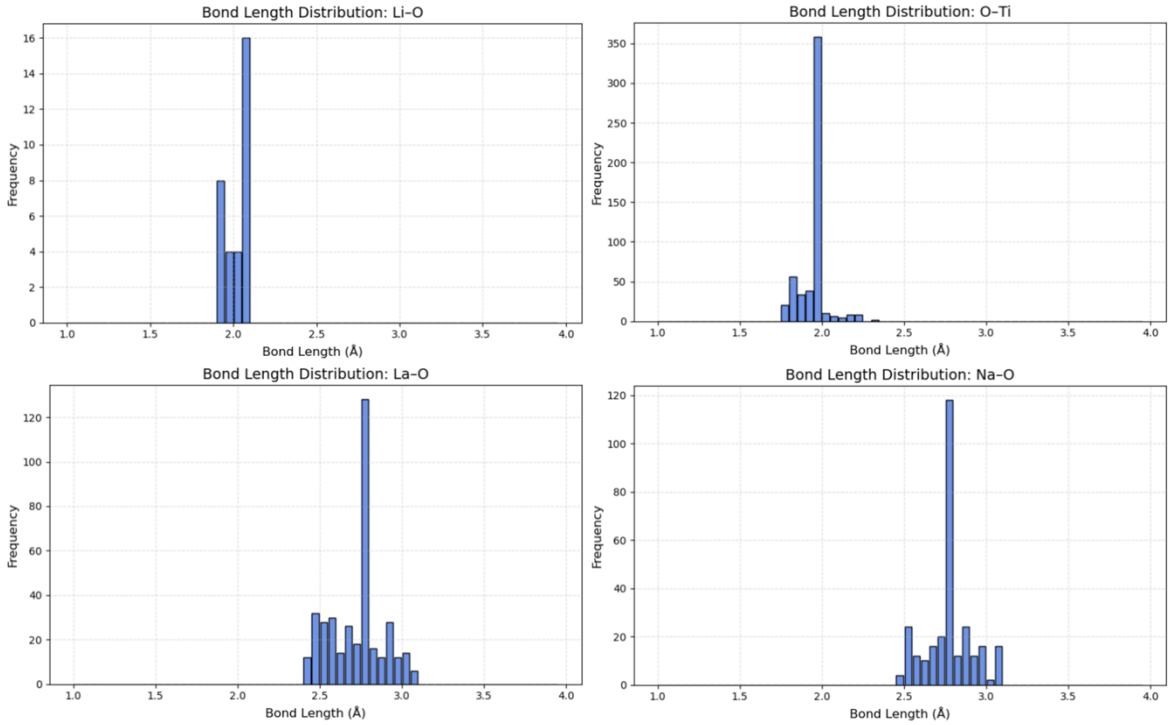

Figure S30. Bond length distributions for Li-O, Na-O, La-O, and Ti-O for surface pseudocubic $Li_{0.125}Na_{0.375}La_{0.5}TiO_3$.

x = 0.50 (Na)

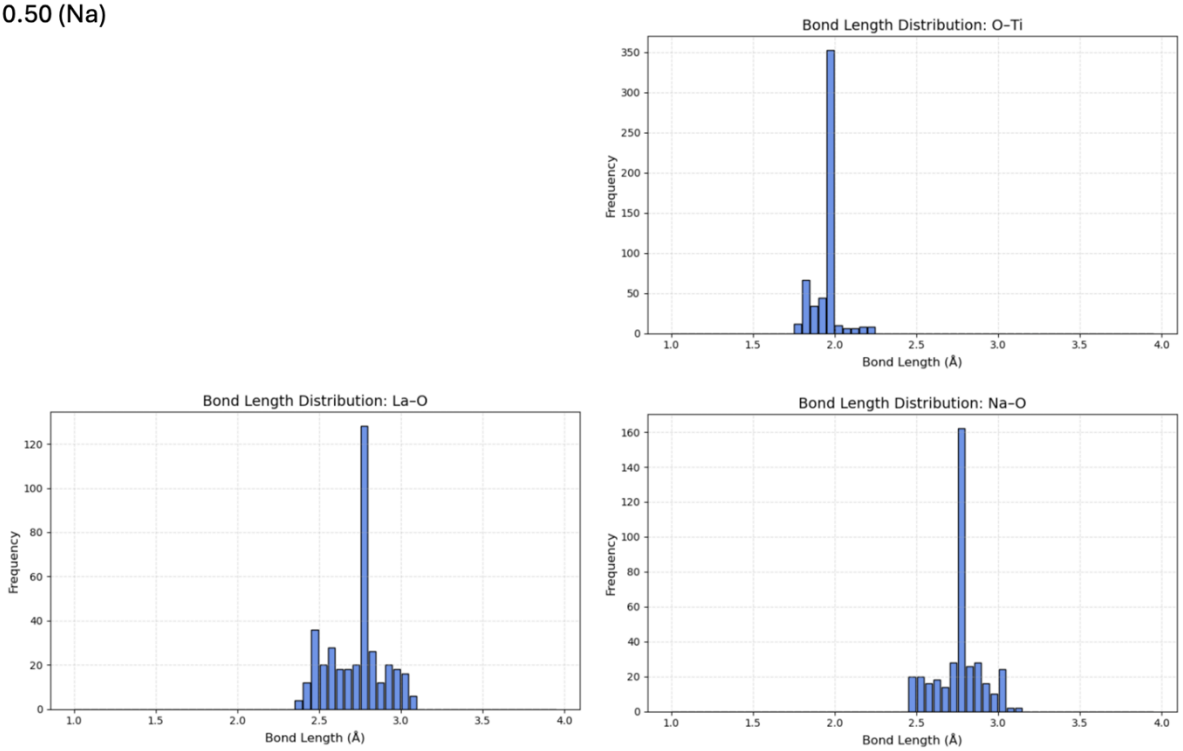

Figure S31. Bond length distributions for Li-O, Na-O, La-O, and Ti-O for surface pseudocubic $Na_{0.5}La_{0.5}TiO_3$.

Average Bond Lengths from LMTO Surface Calculations

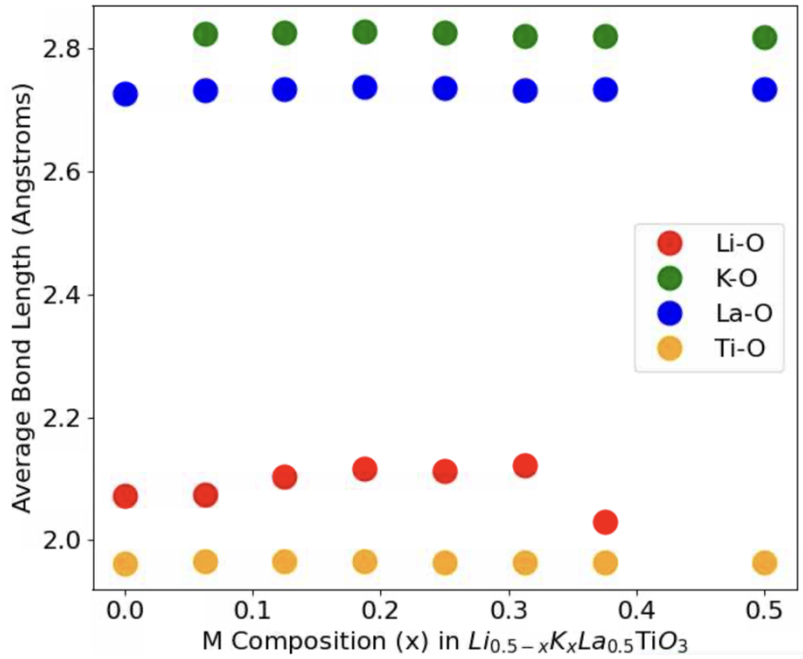

Figure S32. Average bond lengths for Li-O, K-O, La-O, and Ti-O from surface pseudocubic calculations for $Li_{0.5-x}K_xLa_{0.5}TiO_3$, with x varying from 0 to 0.375.

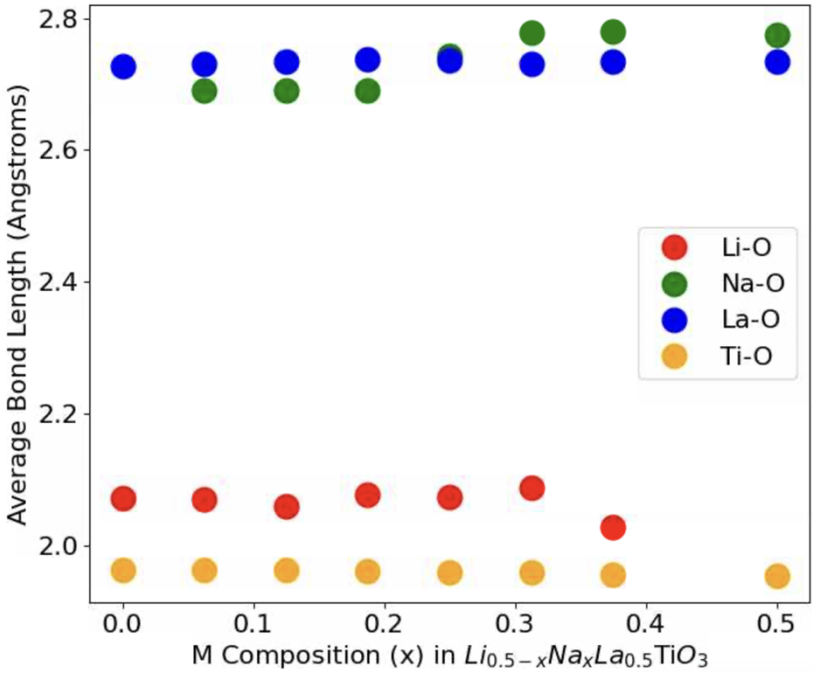

Figure S33. Average bond lengths for Li-O, Na-O, La-O, and Ti-O from surface pseudocubic calculations for $Li_{0.5-x}Na_xLa_{0.5}TiO_3$, with x varying from 0 to 0.375.

TiO_6 Octahedral Rotation Angles from LMTO Surface Calculations

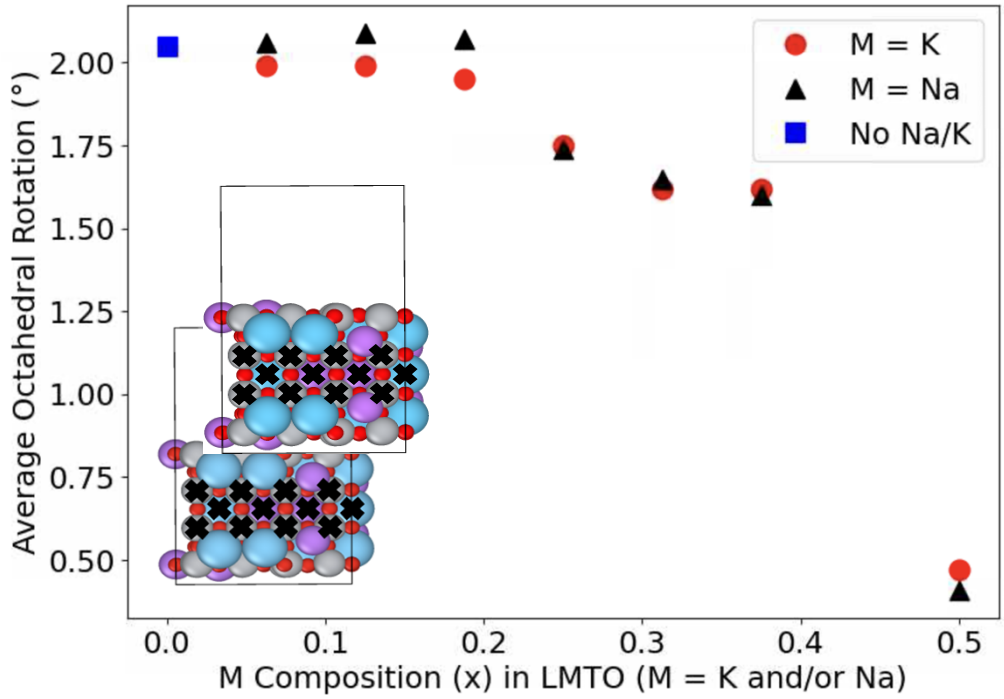

Figure S34. Calculated average TiO_6 octahedral rotation angles with standard deviation error bars from DFT calculations with $Li_{0.5}M_xLa_{0.5-x}TiO_3$ (M = Na or K) ceramic slabs with various M A-site compositions (x). Note that for these calculations, the layers of atoms marked with an × in the structure on the plot were held constant at approximately 0° octahedral rotations, skewing the average octahedral rotation angle values lower.

Calculated Surface Energy from LMTO Surface Calculations

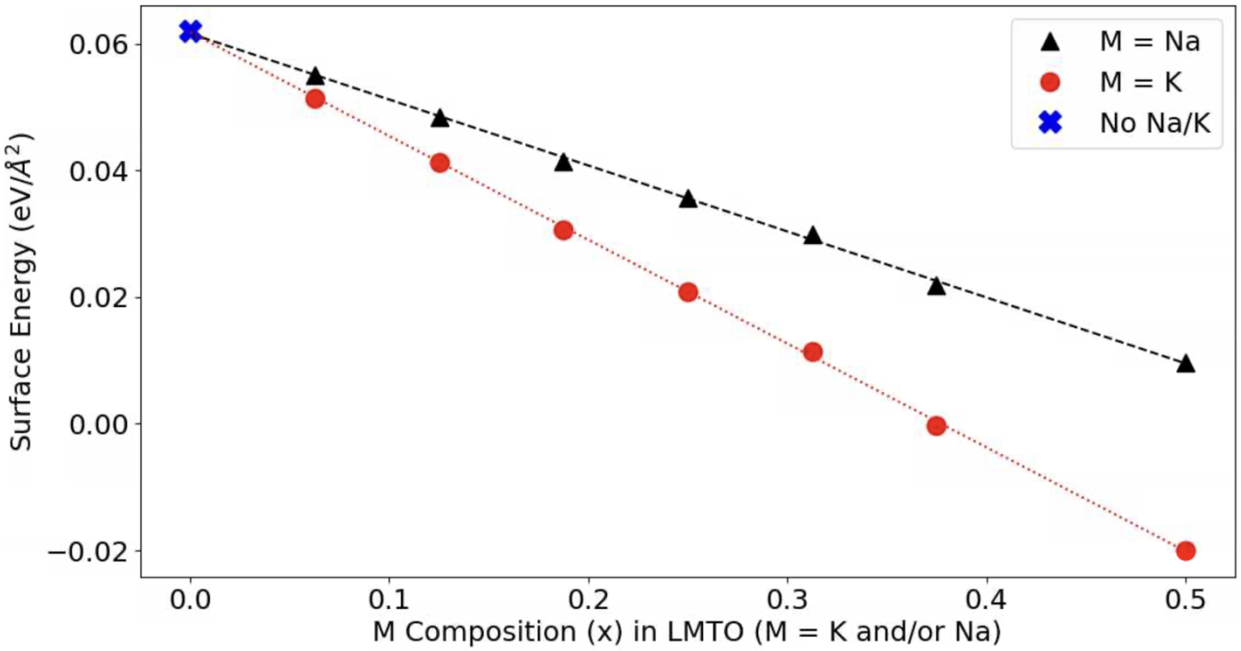

Figure S35. Calculated surface energies (γ) from DFT surface calculations with $Li_{0.5}M_xLa_{0.5-x}TiO_3$ (M = Na or K) ceramic slabs with various M A-site compositions (x).

LiMTFSI Adsorption Energy from LMTO Surface Calculations

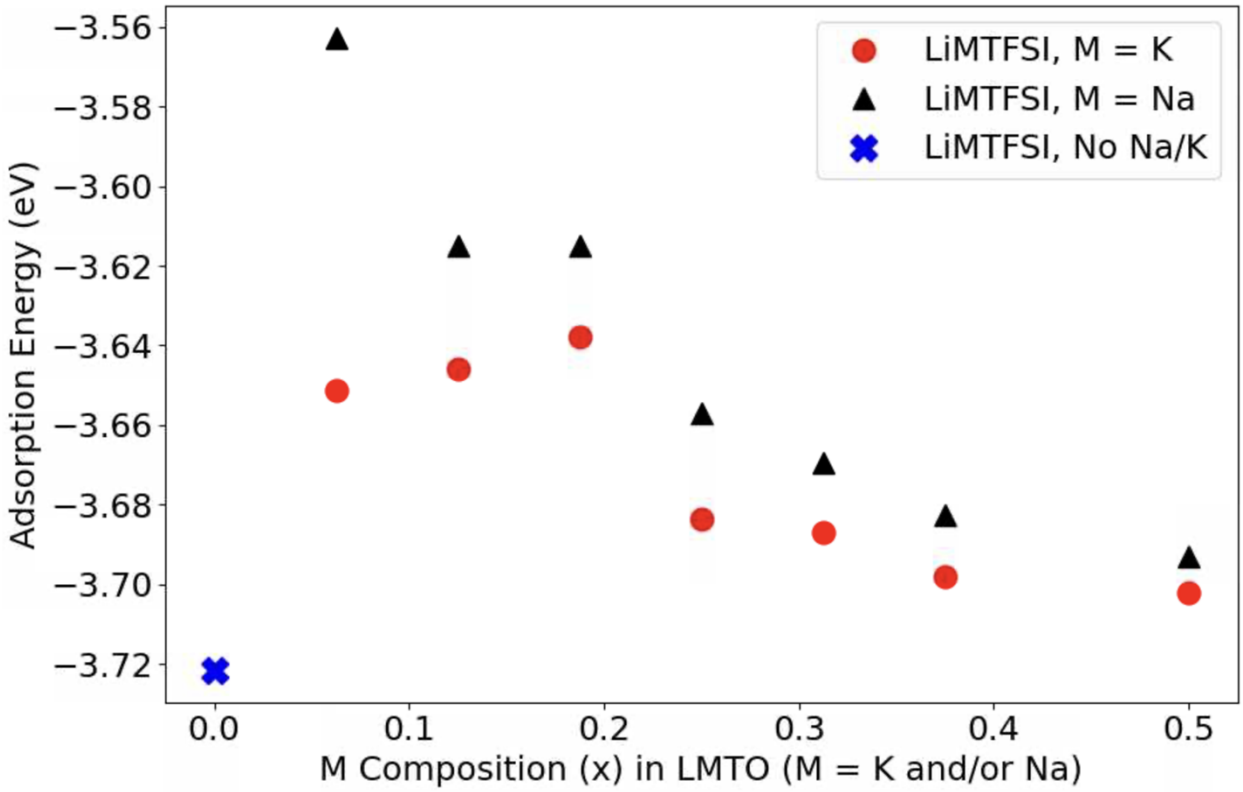

Figure S36. Calculated LiMTFSI adsorption energy $(E_{ads}(LiMTFSI))$ from DFT calculations with $Li_{0.5}M_xLa_{0.5-x}TiO_3$ (M = Na or K) ceramic slabs with various M A-site compositions (x).